Nucleon Decay:

Theory and Experimental Overview

Shunichi Mine
Kamioka Observatory
ICRR, The Univ. of Tokyo
Hida, Japan
mine@km.icrr.u-tokyo.ac.jp
Physics and Astronomy
University of California, Irvine
Irvine, USA
smine@uci.edu

***Abstract*—This article summarizes nucleon decay beyond the Standard Model of particle physics. I briefly explain the theoretical background why the search for nucleon decay is important in the development of particle physics. I also describe the outline and current status of experiments for searching for nucleon decay using Super-Kamiokande. Finally, I describe the prospects of the searches including future experiments.**

Keywords—Nucleon Decay, Proton Decay, Grand Unified Theories, Charge Quantization, Unification of Forces, Super-Kamiokande, Hyper-Kamiokande, DUNE, JUNO, THEIA

I. GRAND UNIFIED THEORIES

One way to extend the Standard Model (SM) of particle physics and incorporate it into a more fundamental theory is to attempt a further unified theory. Remarkably, it is possible to build models that unify not only quarks and leptons, but also electroweak and strong forces. At the same time, some fundamental questions can be answered. Such attempts are called Grand Unified Theories (GUTs) [1].

A. Charge Quantization

In the SM, electromagnetic interactions belong to the $U(1)$ gauge group. The field equation is linear and the normalization of the coupling constant is arbitrary. In other words, the electric charge has no compelling reason to be quantized. However, we know that protons and electrons have the same magnitude of electric charge, and quarks have an integer multiple of 1/3 of it. These facts strongly suggest that charge quantization is a built-in structure of particle theories.

This can be achieved by requiring that the electric charge is a conserved quantity made of group generators of a large symmetry group that can contain the SM. Taking the $SU(5)$ GUT [2] as an example, we can fit the 15 fermions of each generation into $\mathbf{5}$ and $\mathbf{10}$ representations. If the two $SU(5)$ generators are the hypercharge of $U(1)$ and T_3 of $SU(2)$, both are traceless, so the electric charge must also be traceless. This is in sharp contrast to the SM, which has no constraints on hypercharges or charges. Due to the traceless condition, the sum of the charges of each multiplet must be zero, and putting quarks and leptons into the same multiplet forces charge quantization.

The many similarities between quarks and leptons suggest that they can be put into representations of larger symmetry groups, and thus the relationships between them are a theoretical consequence. Just as the $SU(2)$ representation begins with a doublet, the $SU(5)$ representation begins with a 5-component multiplet:

$$SU(2): \begin{pmatrix} \nu_e \\ e^- \end{pmatrix}_L$$

$$SU(5): \begin{pmatrix} \nu_e \\ e^- \\ \bar{d}_r \\ \bar{d}_g \\ \bar{d}_b \end{pmatrix}_L$$

The top two states are the $SU(2)_L$ doublet. The bottom three states are the $\bar{d}_L$ color triplet. There will be operators to raise or lower each state in the $SU(5)$ multiplet. They should not change the spin projection (left-handed). $\bar{d}_L$ is the $SU(2)$ singlet.

The generators of the $SU(n)$ transformations are traceless. Diagonal generators have eigenvalues as the diagonal elements and the trace must be the sum of those eigenvalues, which must be zero. This is familiar in angular momentum. The sum of the eigenvalues of the diagonal generator is always zero. The electric charge operator is a linear combination of $SU(2)$ and $U(1)$ diagonal generators:

$$Q = T_3 + \frac{Y}{2}$$

Therefore, the sum of the electric charge eigenvalues is zero. This implies that the sum of the electric charges of neutrino, electron, and three $\bar{d}$ is zero, thus leading to the electric charge of $\bar{d}$ being 1/3:

$$Q(\nu_e) + Q(e^-) + 3Q(\bar{d}) = 0$$

The fractional charge of quarks is related to the number of colors. This also explains why the electric charges are quantized and why the absolute values of the electron and proton charges are the same and therefore the atoms are neutral.

B. Unification of Forces

There are 19 parameters which have to be fitted to data in the SM: Three gauge couplings, α_1, α_2 and α_3, 13 parameters associated with the Yukawa couplings, the Higgs mass and

quartic coupling, and θ_{QCD}. The coupling α_1, α_2 and α_3 approximately satisfies the following equation:

$$\frac{1}{\alpha_i(M^2)} = \frac{1}{\alpha_i(\mu^2)} + \frac{b_i}{4\pi}\ln\frac{M^2}{\mu^2}$$

$$b_1 = \frac{-2n_f}{3}$$

$$b_2 = \frac{22}{3} - \frac{2n_f}{3}$$

$$b_3 = 11 - \frac{2n_f}{3}$$

where M is the mass scale or momentum transfer scale at which we want to calculate α_i, μ is the scale where the coupling is measured, and b_1, b_2 and b_3 are for the $U(1)$, $SU(2)$ and $SU(3)$ interactions. n_f is the number of flavors with mass $m_f \lesssim M$ so that they enter the loop in Fig. 1.

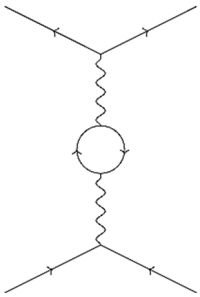

Fig. 1. One-loop Feynman diagram.

These virtual diagrams cause the couplings to be a function of energy scale. The negative contributions in the equations for b_2 and b_3 arise from fermion loops and the positive contributions from the gauge boson loops (Fig. 2).

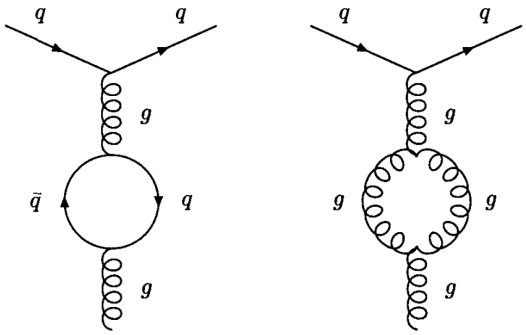

Fig. 2. One-loop Feynman diagram. They are examples involving gluons.

Each GUT has some new particle loop and slightly different b_i. Since the α_i vary differently depending on the energy scale, we can ask if they are equal at a certain mass.

Using two of the three equations for α_i, M_{unif} can be determined:

$$\ln\frac{M_{unif}}{\mu} = \frac{6\pi}{11}\left(\frac{1}{\alpha_2(\mu^2)} - \frac{1}{\alpha_3(\mu^2)}\right)$$

If we take $\mu = M_W$, $\alpha_2 = 1/30$, and $\alpha_3 = 0.11$, M_{unif} is approximately 10^{17} GeV. Note that M_{unif} depends exponentially on α_i and is also sensitive to radiative corrections. If the couplings come together, it occurs at a very large energy scale or a very short distance. Each $1/\alpha_i$ is a linear function of $\ln M_{unif}/\mu$ as shown in Fig. 3.

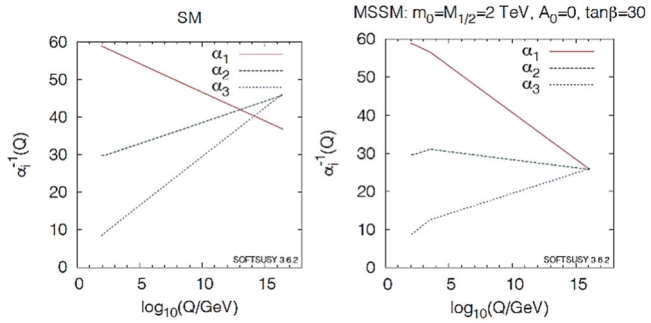

Fig. 3. Running couplings in SM and MSSM (Minimal Supersymmetric Standard Model) [1].

These slopes depend on b_i determined by the particular group structure and gauge field. Using the value of α_i measured, for example, at M_Z, it is possible to calculate whether these slopes converge at one point.

In a supersymmetric (SUSY) $SU(5)$ GUT [3], these couplings meet at a single point within the accuracy of the measurement of α_i at M_Z. In supersymmetric theory, the superpartners also enter the loops and change b_i. The following ratio, which combines the running equations, can be used to investigate which theories unify the couplings:

$$\frac{\alpha_i^{-1}(\mu) - \alpha_j^{-1}(\mu)}{\alpha_j^{-1}(\mu) - \alpha_k^{-1}(\mu)} = \frac{b_i - b_j}{b_j - b_k}$$

The left-hand side is estimated from data, and the right-hand side is found by different theories. The LEP data at M_Z gives 1.37 ± 0.07 on the left-hand side [4]. In the SM, the right-hand side is 1.90. The unification is therefore approximate. In the supersymmetric extension, including the superpartners in the loops and the need for two Higgs doublets, the right-hand side is 1.4. This is consistent with the LEP data. Within experimental errors, the supersymmetric extension of the SM unify the couplings.

C. Nucleon Decay

When ν_e and e^- are put in the $SU(2)$ doublet, the gauge bosons $W^\pm$ act as "raising" or "lowering" operators causing transitions between them. Similarly, when quarks and leptons are put into the $SU(5)$ multiplet, $SU(5)$ gauge bosons arise. Some of those gauge bosons are the familiar γ, $W^\pm$, Z, and gluon, and the rest bosons can cause transitions between quarks and leptons within the multiplet. If the quarks in a nucleon can turn to leptons, the nucleon can decay and baryon number is no longer conserved.

By analogy to smaller groups, let us find the quantum numbers of those new bosons. In $SU(2)$, the gauge bosons coupled by the fermions in doublets have $\mathbf{2} \times \overline{\mathbf{2}} = \mathbf{1} + \mathbf{3}$ and the Ws belong to the triplet. In $SU(3)$, the gauge bosons have $\mathbf{3} \times \overline{\mathbf{3}} = \mathbf{1} + \mathbf{8}$ and the gluons belong to the octet. In $SU(5)$, the gauge bosons have $\mathbf{5} \times \overline{\mathbf{5}} = \mathbf{1} + \mathbf{24}$. Recalling that the $\mathbf{5}$ contains $(2,1) + (1,3)$, we can find the quantum numbers of the new bosons. Here, the quantities in brackets are $(SU(2)\text{ multiplicity}, SU(3)\text{ multiplicity})$. $\overline{\mathbf{5}}$ contains $(\overline{2}, 1) + (1, \overline{3})$. Therefore, $\mathbf{5} \times \overline{\mathbf{5}}$ contains:

$$(2 \times \bar{2}, 1) + (1,3 \times \bar{3}) + (2, \bar{3}) + (\bar{2}, 3)$$
$$= (1,1) + (3,1) + (1,1) + (1,8) + (2, \bar{3}) + (\bar{2}, 3).$$

The singlet under both $SU(2)$ and $SU(3)$ is $\mathbf{1}$ in $\mathbf{1} + \mathbf{24}$, and changes no quantum numbers. The $(3,1)$ and $(1,1)$ are the Ws and B, and the $(1,8)$ are the gluons. The remaining states, an $SU(2)$ doublet of color triplets and their antiparticles, are the new bosons. They are usually denoted as $(Y\ X)$ with electric charges $Q_Y = -1/3$, $Q_X = -4/3$. The new vertices are shown in Fig. 4.

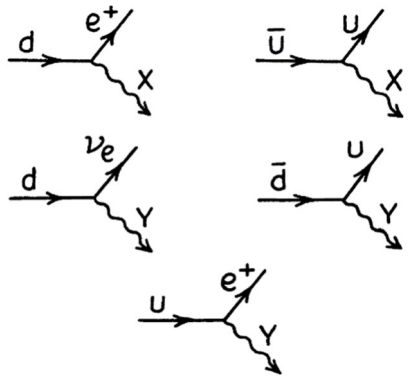

Fig. 4. New vertices with X and Y gauge bosons.

The lines can be reversed by replacing particle and antiparticle. Any process can occur with vertices of the SM plus these.

One possible nucleon decay process is shown in Fig. 5.

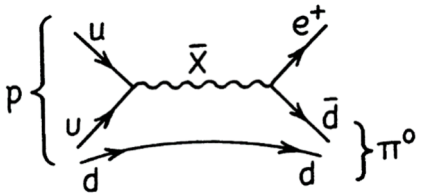

Fig. 5. An example of Feynman diagram of $p \to e^+\pi^0$.

This $p \to e^+\pi^0$ is the dominant nucleon decay mode predicted by many GUTs such as the minimal $SU(5)$ and $SO(10)$ [5] models, which is not allowed in the SM. M_X is probably very large, on the order of the grand unification scale, and the decay width can be crudely estimated. The matrix element must have a factor ${g_5}^2/{M_{unif}}^2$, so the width has a factor ${g_5}^4/{M_{unif}}^4$. Considering the dimensions, the width must be proportional to a mass, and the proton mass m_p is the only relevant. Therefore, the width Γ must be about:

$$\Gamma_{p \to e^+\pi^0} \approx \frac{{g_5}^4 {m_p}^5}{{M_{unif}}^4}$$

The numerical factor should be proportional to the probability of two quarks being in the same place so they can annihilate. The lifetime $\tau_p = 1/\Gamma_p$ should be even longer than indicated by the width shown above. Since τ_p varies in proportion to M_{unif}, it is very sensitive to the value of M_{unif}. For $M_{unif} = 5 \times 10^{15}$ GeV, τ_p is about 10^{31} years. Since the lifetime of the universe is about 10^{10} years, although protons would not be stable, they would appear very stable compared to the scale of the lifetime of the universe. This is consistent with our perception of them as stable.

One of the outstanding mysteries in modern physics is the dominance of matter over antimatter in the universe. Assuming that the particles we see today are created by the same physics as we currently know, the total baryon number would be expected to be zero, since matter and antimatter should be produced in equal amounts. Most GUTs predict baryon number violation (BNV), which is one necessary condition for this matter dominance [6].

D. Representative GUTs

Early simpler GUTs including minimal $SU(5)$ (the Georgi-Glashow model) have already been ruled out experimentally. This subsection introduces some representative GUTs based on symmetries larger than simple $SU(5)$. They predict longer nucleon decay lifetimes.

Although the $SU(5)$ model proposes the minimal GUT, the unification is far from complete. For one generation of fermions in the SM, two independent representations, **5** and **10**, are required. For right-handed neutrino a $SU(5)$ singlet must be added. In this case, the right-handed neutrino mass is not necessarily related to the GUT scale. By contrast, a single 16-dimensional spinor representation of $SO(10)$ accommodates all SM fermions together with an extra singlet, potentially providing the right-handed neutrino. This can be understood from the breaking pattern $SO(10) \to SU(5) \times U(1)_X$ and the associated branching rule $\mathbf{16} = \bar{\mathbf{5}} + \mathbf{10} + \mathbf{1}$ [7]. One generation of quarks and leptons appear in the **16** as shown in Fig. 6.

state	Y	Color	Weak	$SU(5)$	$SO(10)$
ν^c	0	$---$	$--$	**1**	
e^c	2	$---$	$++$		
u_r	1/3	$+--$	$-+$		
d_r	1/3	$+--$	$+-$		
u_g	1/3	$-+-$	$-+$		
d_g	1/3	$-+-$	$+-$	**10**	
u_b	1/3	$--+$	$-+$		
d_b	1/3	$--+$	$+-$		**16**
u_r^c	−4/3	$-++$	$--$		
u_g^c	−4/3	$+-+$	$--$		
u_b^c	−4/3	$++-$	$--$		
d_r^c	2/3	$-++$	$++$		
d_g^c	2/3	$+-+$	$++$		
d_b^c	2/3	$++-$	$++$	$\bar{\mathbf{5}}$	
ν	−1	$+++$	$-+$		
e	−1	$+++$	$+-$		

Fig. 6. Quantum numbers of 16-dimentional representation of $SO(10)$ [1].

The first three ("Color") and last two ("Weak") spins correspond to $SU(3)_c$ and $SU(2)_L$, respectively. The $SO(10)$ GUT has multiple routes that break the symmetry and can adjust the evolution of the running couplings. For instance, it is possible to have the three couplings meet and to reproduce the observed nucleon decay rate limit.

Adding supersymmetric particles not only matches the three couplings, but also increases the energy scale of the unification as shown in Fig. 3. Therefore, the nucleon decay lifetime expected from SUSY GUTs is longer. However, in SUSY GUTs, there are additional sources for BNV dimension-five operator. The dimension-five operators have a dimensionful coupling of order $(1/M_{unif})$. The dominant decay mode from dimension-five operators is $p \to \bar{\nu}K^+$.

Because a second or third generation particle must appear in the final state from a symmetry argument of the operators with bosonic superfields [8]. Supersymmetry could also allow a natural large hierarchy in energy separating the electroweak scale from the Grand Unified scale.

Theoretical predictions of proton lifetime for representative GUT models are shown in Fig. 7.

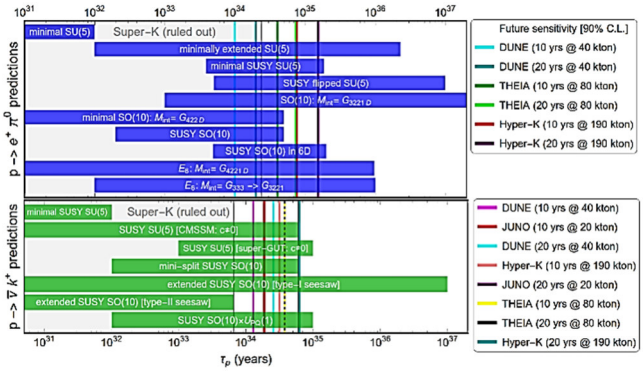

Fig. 7. Theoretical predictuions of proton lifetime for representative GUT models [9]. Current Super-Kamiokande data rule out the gray shaded regions. Future sensitivities from Hyper-Kamiokande, DUNE, JUNO, and THEIA are also shown.

It is worth noting that none of the predictions are sharp. Typically, the predicted range of each theory spans several orders of magnitude. This is associated with a number of theoretical uncertainties that affect the precision of the calculations at various levels. Therefore, it is important to search for as many baryon number violating channels as possible experimentally.

II. EXPERIMENTS

Starting with the IMB, Kamiokande, Frejus, and Soudan experiments in the 1980s [10], searches for various modes of nucleon decay have continued to be actively conducted to date, but no significant signal exceeding background has so far been observed. For most decay modes, the lower limits of lifetime have been determined from Super Kamiokande (SK) experiment [11]. A comparison between the lower limits of the lifetime measured by SK and the lifetime predicted by various theories for two benchmark decay modes, $p \to e^+\pi^0$ and $p \to \bar{\nu}K^+$, is shown in Fig. 7. The current experimental searches are in the interesting ranges.

This chapter summarizes the experimental outline using SK and the latest results from SK. The outline of the nucleon decay search experiment will be explained using $p \to e^+\pi^0$ mode as the example unless otherwise specified. We also discuss future experiments currently planned to further increase the lifetime measurement sensitivities.

A. Principle and Method

A typical $p \to e^+\pi^0$ event simulated in SK is shown in Fig. 8.

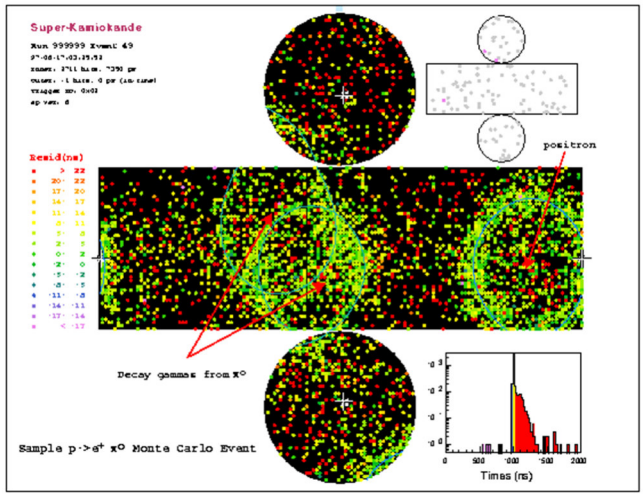

Fig. 8. A typical $p \to e^+\pi^0$ simulated event in SK [12].

The positron produces an electromagnetic shower, which is balanced by two electromagnetic showers from the instantaneous decay of the π^0.

To search for nucleon decay, it is necessary to get together a large number of nucleons and carefully observe them. One cubic centimeter of water contains about 6×10^{23} nucleons. Therefore, a 10 m cube contains about 10^{33} nucleons. SK is the world's largest water tank Cherenkov detector. The SK detector consists of a vertical cylindrical tank, 39 m in diameter and 42 m in height. A typical fiducial volume ("conventional FV": defined as the distance from the reconstructed vertex to the nearest inner detector, ID, wall being greater than 2 m) used in physics data analysis contains approximately 7.5×10^{33} protons and 6.0×10^{33} neutrons.

The combination of a transparent medium such as water with photomultiplier tubes (PMTs) as light sensors is beneficial for achieving a large effective volume at a low cost. Such as medium serves as a target for nucleon decays and is well suited for propagating Cherenkov light from charged final-state particles and energetic photons. A water purification system can remove radioactive substances and impurities and constantly circulate ultrapure water in the tank. The attenuation of light due to absorption and scattering in water is measured as a function of wavelength as shown in Fig. 9.

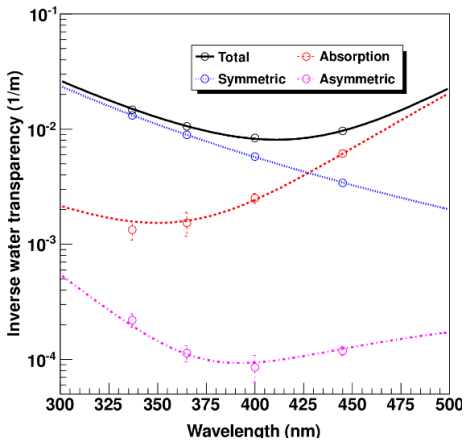

Fig. 9. Typical fitted water coefficient functions used in the SK detector simulator [11]. The points are the data obtained in April 2009.

Symmetric (Rayleigh) scattering is dominant at shorter wavelengths and absorption is dominant at longer wavelengths. The light transmittance is highest at around 400 nm, matching the maximum quantum efficiency of the photocathode of the SK PMTs. At this wavelength the water transparency is approximately 100 m.

The SK detector cavity lies under the peak of Mt. Ikenoyama, with 1,000 m of rock (2,700 m.w.e.) mean overburden (Fig. 10).

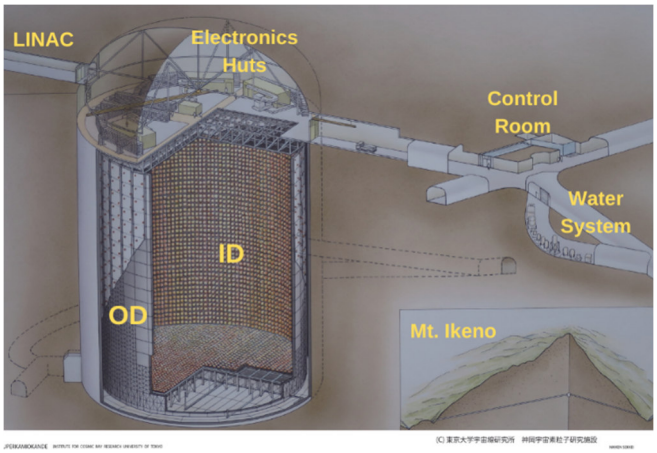

Fig. 10. A scketch of the SK detector site (Figure courtesy: Kamioka Observatory, ICRR, The University of Tokyo.)

Cosmic ray muons with energy of less than 1.3 TeV cannot penetrate to a depth of 2,700 m.w.e. The observed muon flux, which does not pose a significant background for the experiment, is 6×10^{-8} cm^{-2} s^{-1} sr^{-1}. In addition, the outer detector (OD) absorbs or discriminates against incoming background particles from outside. Atmospheric neutrinos are a background for the nucleon decay search.

The detector water is contained in a tank lined with PMTs. For each event, the number of photons and time information for each PMT is recorded. The Cherenkov light produced by a charged particle is reconstructed as a ring of hit PMTs. Cherenkov light is emitted in a cone shape, surrounding the direction of the charged particle. The energy, direction, particle type, and so on. are determined using information obtained from the PMTs, such as the amount of light detected and the ring shape [13]. Muons are basically single particles and make sharp rings, whereas electrons, positrons, and gamma ray photons initiate electromagnetic showers and the nearly parallel electrons and positrons in the shower combine to make a fuzzy ring, as shown in Fig. 11.

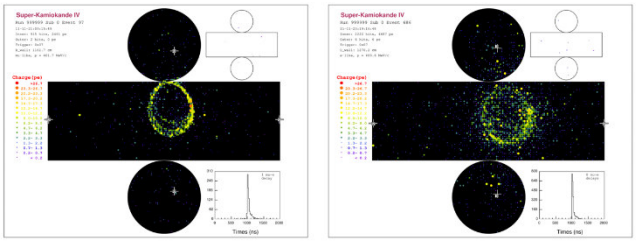

Fig. 11. A typical muon (left) and an electron (right) simulated events in SK (Figure courtesy: Kamioka Observatory, ICRR, The University of Tokyo.)

Coulomb scattering of the electron also contributes to the fuzziness of the ring. The excellent PID performance (e/μ separation) was experimentally confirmed using a 1-kiloton (KT) water Cherenkov detector with electron and muon beams from the 12 GeV proton synchrotron at KEK [14]. When multiple Cherenkov rings are observed, the direction, the particle type, and momentum are obtained for each ring, as in the case of the single ring event. Fig. 12 shows a typical reconstructed invariant mass distribution of the neutral pion events produced by atmospheric neutrino interactions.

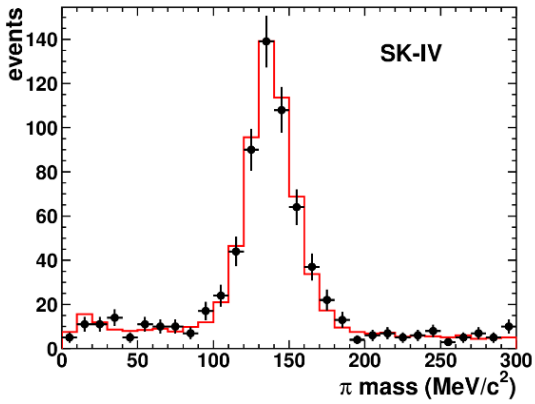

Fig. 12. Reconstructed invariant mass distribution of the atmospheric-neutrino-induced π^0 events in the observed data (dot) and simulated samples (histogram) in SK [15].

The difference between the data and simulation peaks is used to estimate the absolute energy scale uncertainty. By assuming a type of nucleon decay, measurements of each charged particle in the final state can be used to reconstruct the original nucleon mass, and so on. In high energy physics (above about 0.1 GeV) data analysis, we use events above the energy threshold of several tens of MeV, so a few MeV radioactivity is not a background.

Fig. 13 summarizes each detector phase of the SK experiment.

Detector phase (years)	Live time [days]	Exposure [kt·yrs] Conv. FV / Exp. FV		ID PMT photo-coverage [%]	ID PMT cover	ID readout elec. modules	Gd-loading	Gd-n capture efficiency [%]
I (1996–2001)	~1489	~92	~111	~40		ATM		N/A
II (2002–2005)	~799	~49	~59	~20	✓	ATM		N/A
III (2006–2008)	~518	~32	~39	~40	✓	ATM		N/A
IV (2008–2018)	~3244	~200	~241	~40	✓	QBEE		N/A
V (2019–2020)	~461	~28	~34	~40	✓	QBEE		N/A
VI (2020–2022)	~564	~35	~42	~40	✓	QBEE	✓	~50
VII (2022–)	on-going	on-going	on-going	~40	✓	QBEE	✓	~75

Fig. 13. Summary of the SK detector phases [11,16].

So far, published nucleon decay search results have been obtained using data up to the pure water phases (SK I−V), before loading gadolinium. In the phases with gadolinium (SK VI[16] −VII), the neutron capture efficiency is higher, and it is expected that atmospheric neutrino background events accompanied by neutron production would be reduced further. Data analysis using the expanded fiducial volume ("expanded FV": defined as the distance from the reconstructed vertex to the nearest ID wall is greater than 1 m) in the pure water phase alone has already accumulated an exposure approaching half a megaton-years.

Lifetime sensitivity is approximately proportional to $\varepsilon \cdot VT$ for the background-free case and $\left(\varepsilon/\sqrt{N_{bkg}}\right) \cdot \sqrt{VT}$ for the background-dominant case. Here, ε is the signal detection

efficiency, V is the fiducial volume, T is the measurement time, and N_{bkg} is the number of expected background events. The detector must have good sensitivity to Cherenkov photons and high detection efficiency to nucleon decay signal events. Additionally, it is necessary to efficiently reduce the atmospheric neutrino background events. Furthermore, it is important to reduce systematic errors in detection efficiency and expected number of background events, respectively.

The $p \rightarrow e^{+}\pi^{0}$ candidate events are searched by the following sequence of event selections [17]:

- Events must be "fully-contained" (There is no activity in the OD indicating entering or exiting particles.) with a reconstructed vertex within the fiducial volume.
- Events must have two or three reconstructed Cherenkov rings.
- All rings must be reconstructed as showering.
- There must be no tagged Michel electrons.
- The total reconstructed mass must be between 800 and 1050 MeV/c^2.
- The total reconstructed momentum must be less than 250 MeV/c.
- There must be no tagged neutrons (from SK-IV).

As for the example, the total reconstructed mass distributions after applying all the selection cuts have been applied except the cut on the total mass are shown in Fig. 14.

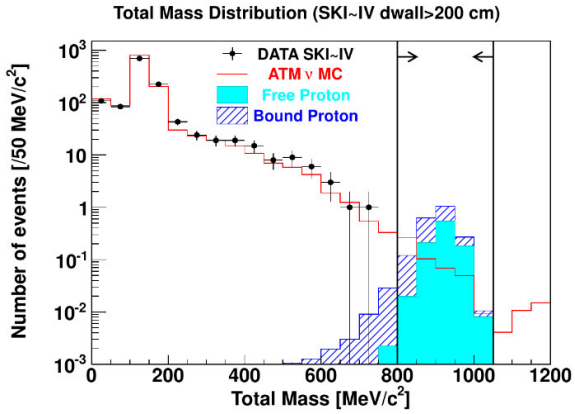

Fig. 14. Reconstructed total mass distributions for the conventional FV [17].

Free protons are well reconstructed around the expected proton mass. The kinematics of bound proton decays suffer pion scattering or correlated decay and therefore the reconstructed mass distribution is broader. The data distribution is well reproduced by atmospheric neutrino background MC. There are no data events in the signal region. The signal selection efficiencies and the expected number of atmospheric neutrino background events and data candidates for the conventional FV are shown at each step of the selection in Fig. 15.

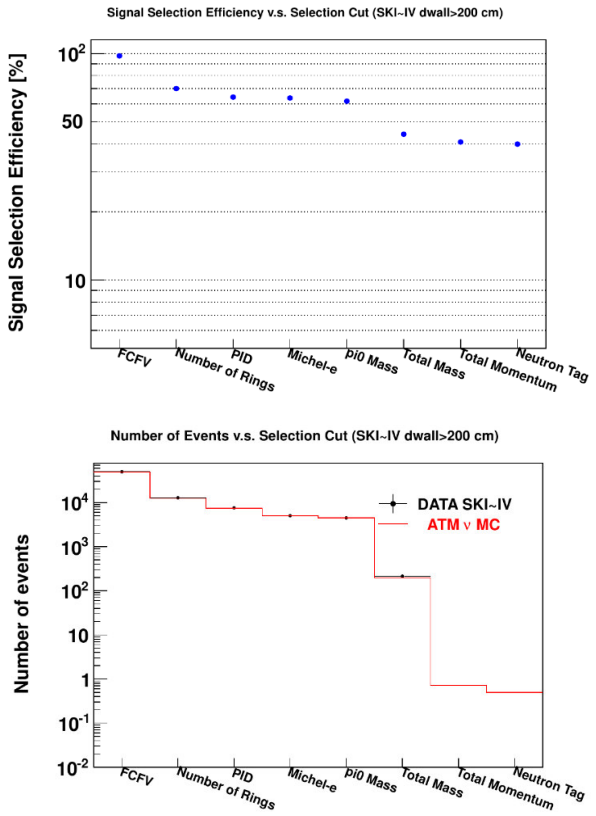

Fig. 15. The signal efficiencies (upper) and the expected number of atmospheric neutrino background events and data candidates (lower) for the conventional FV [17].

The livetime-weighted total signal selection efficiency and expected number of background events are ~40% and ~0.5 events, respectively. As the expected number of background events is less than 1, statistical errors are dominant, so the contribution of systematic errors becomes small. Therefore, in data analysis counting the number of signal candidate events, suppressing the number of expected background events to 1 or less is one criterion for optimizing event reconstruction and event selections.

B. Experimental Check of Atmospheric Neutrino Background

Atmospheric neutrinos are a background for the nucleon decay search as the neutrino interactions produce charged particles and energetic photons, sometimes kinetically indistinguishable from the nucleon decay signal. Charged-current (CC) interaction of atmospheric ν_e with only an electron and single π^0 in the final state are the dominant source of the background to $p \rightarrow e^{+}\pi^{0}$ search. Parent neutrino energies between 1 and 3 GeV dominate for the background events. It is essential to experimentally check the neutrino interactions and the interactions of generated particles in oxygen nuclei and in water, which are used in atmospheric neutrino background simulations [18].

The wideband neutrino beam used in the K2K long-baseline neutrino oscillation experiment [19] was primarily muon flavored (about 97% for ν_μ) with a mean energy of 1.3 GeV. The K2K experiment used a 1-kiloton (KT) water Cherenkov detector located at about 300 m from an aluminum neutrino production target. The vertical cylindrical tank (~11 m in diameter and ~11 m in height), the PMT type,

the photo-coverage (~40%), the water purification system, the readout electronics, the event reconstruction algorithm, and the detector calibration methods were basically the same as those in SK. While the KT detector measures muon neutrino reactions rather than electron neutrino reactions, the dynamics of pion production and rescattering processes in the oxygen nucleus are identical between the two neutrino flavors. Therefore, rare CC ν_e interaction topologies which may mimic proton decay can be checked using the KT detector ν_μ events with a muon and single π^0 in the final state. The K2K KT detector, with the same target material and detection technique as SK, accumulated data equivalent to atmospheric neutrino exposures of 15.9 and 4.5 megaton-years for the CC and neutral-current (NC) background events, respectively.

The total mass distributions for "$\mu\pi^0$" events, selected with nearly the same cuts used for the SK $p \to e^+\pi^0$ search except for the choice of lepton PID ("muon-like"), are shown in Fig. 16.

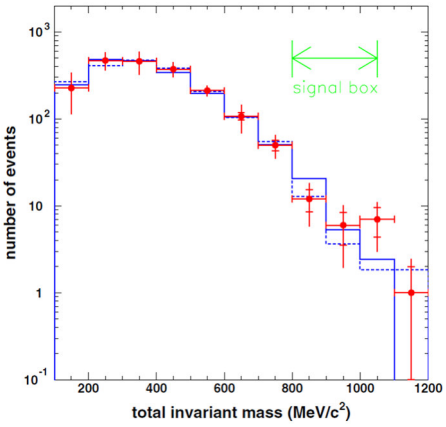

Fig. 16. Reconstructed total mass distributions for "$\mu\pi^0$" events with reconstructed total momentum is less than 250 MeV/c [18]. Red crosses show the data with statistical and total measurement errors. The NEUT and NUANCE predictions are shown by a solid and dashed histogram, respectively.

The data and simulations used in the SK nucleon decay searches agree well including the tails of distributions where the proton decay signal box is located.

A total of 24 "proton decay"-like events were identified in the KT data. The expected event rate of the $p \to e^+\pi^0$ background for general water Cherenkov detectors, N, can be expressed as $N = n \cdot R_\phi \cdot R_\varepsilon$, where n is the observed events in the proton decay signal box at the KT, R_ϕ is a ratio of total neutrino interactions between the atmospheric neutrinos at the proton decay detectors and the K2K muon neutrinos at the KT, and R_ε is the ratio of detection probabilities for the background events at the proton decay detectors and the KT. In the SK's $p \to e^+\pi^0$ search, the expected atmospheric neutrino background rate (without the tagged neutron cut for the conventional FV) estimated with MC is 1.84/megaton-years [17]. This is consistent with the measurement result by the K2K KT detector of $1.63^{+0.42}_{-0.33}(\text{stat})^{+0.45}_{-0.51}(\text{syst})$ / megaton-years from the neutrinos whose energies are below 3 GeV.

The KT result shows that about two background events per year would be expected for 1 megaton-years for SK-type water Cherenkov detectors. Assuming a finite proton lifetime by an order beyond the present limit, the rate of signal would be similar to the expected background rate, both in the proposed detectors as well as in a still-running SK. Therefore, further reduction of the background events, such as improved neutron tagging, is crucial to make a clean discovery of proton decay.

C. *Recent results from Super-K*

As shown in Fig. 13, the SK VII experiment is currently on-going. For data analysis in the SK-Gd phase (SK VI−VII), detector calibration, detector simulator and event reconstruction tuning and development are being carried out. Data in the pure water phase (SK I − V) are also being reanalyzed using better data analysis tools on several decay modes.

Although the $p \to e^+\pi^0$ decay mode is predicted to be dominant in many GUTs, a variety of other decay modes are possible, each with a sizable branching ratio. When bound in a nucleus the neutron is stable against weak decay, but it is not protected against baryon number violating decays. The diversity in those predictions suggests that in order to make a discovery and to subsequently constrain nucleon decay models, it is critical to probe as many nucleon decay modes as possible. SK is sensitive to many decay modes beyond the two benchmark decays. So far, no nucleon decay signals have been observed that significantly exceed the expected number of background events. Fig. 17 summarizes the latest lifetime lower limits of the nucleon decay searches at SK.

Decay mode	SK detector	Exposure [kt-years]	Lifetime limit [years]	Reference	Comments
$p \to e^+\pi^0$	I–IV	450	2.4×10^{34}	[20]	Expanded FV
$p \to \mu^+\pi^0$	I–IV	450	1.6×10^{34}	[20]	Expanded FV
$p \to \nu\pi^+$	I–III	173	3.9×10^{32}	[21]	
$n \to \nu\pi^0$	I–III	173	1.1×10^{33}	[21]	
$p \to e^+\eta$	I–IV	373	1.4×10^{34}	In prep.	
$p \to \mu^+\eta$	I–IV	373	7.3×10^{33}	In prep.	
$p \to e^+\rho^0$	I–IV	316	7.2×10^{32}	[22]	A part of SK IV data
$p \to \mu^+\rho^0$	I–IV	316	5.7×10^{32}	[22]	A part of SK IV data
$p \to e^+\omega$	I–IV	316	1.6×10^{33}	[22]	A part of SK IV data
$p \to \mu^+\omega$	I–IV	316	2.8×10^{33}	[22]	A part of SK IV data
$n \to e^+\pi^-$	I–IV	316	5.3×10^{33}	[22]	A part of SK IV data
$n \to \mu^+\pi^-$	I–IV	316	3.5×10^{33}	[22]	A part of SK IV data
$n \to e^+\rho^-$	I–IV	316	3.0×10^{31}	[22]	A part of SK IV data
$n \to \mu^+\rho^-$	I–IV	316	6.0×10^{31}	[22]	A part of SK IV data
$p \to e^+\pi^0\pi^0$	I–V	401	7.2×10^{33}	In prep.	
$p \to \mu^+\pi^0\pi^0$	I–V	401	4.5×10^{33}	In prep.	
$p \to e^+e^+e^-$	I–IV	373	3.4×10^{34}	[23]	
$p \to \mu^+e^+e^-$	I–IV	373	2.3×10^{34}	[23]	
$p \to \mu^-e^+e^+$	I–IV	373	1.9×10^{34}	[23]	
$p \to e^+\mu^+\mu^-$	I–IV	373	9.2×10^{33}	[23]	
$p \to e^-\mu^+\mu^+$	I–IV	373	1.1×10^{34}	[23]	
$p \to \mu^+\mu^+\mu^-$	I–IV	373	1.0×10^{34}	[23]	
$p \to e^+\nu\nu$	I–IV	273	1.7×10^{32}	[24]	A part of SK IV data
$p \to \mu^+\nu\nu$	I–IV	273	2.2×10^{32}	[24]	A part of SK IV data
$p \to e^+X$	I–IV	273	7.9×10^{32}	[25]	A part of SK IV data
$p \to \mu^+X$	I–IV	273	4.1×10^{32}	[25]	A part of SK IV data
$n \to \nu\gamma$	I–IV	273	5.5×10^{32}	[25]	A part of SK IV data
$p \to \nu K^+$	I–IV	365	8.2×10^{33}	[26]	A part of SK IV data
$p \to \mu^+K^0$	I–IV	373	3.6×10^{33}	[27]	
$p \to e^+K^0$	I	92	1.3×10^{33}	[28]	
$p \to \mu^+K^0$	I	92	1.0×10^{33}	[28]	

$pp \to e^+e^+$	I–IV	373	4.2×10^{33}	[29]	
$nn \to e^+e^-$	I–IV	373	4.2×10^{33}	[29]	
$nn \to \gamma\gamma$	I–IV	373	4.1×10^{33}	[29]	
$pp \to e^+\mu^+$	I–IV	373	4.4×10^{33}	[29]	
$nn \to e^+\mu^-$	I–IV	373	4.4×10^{33}	[29]	
$nn \to e^-\mu^+$	I–IV	373	4.4×10^{33}	[29]	
$pp \to \mu^+\mu^+$	I–IV	373	4.4×10^{33}	[29]	
$nn \to \mu^+\mu^-$	I–IV	373	4.4×10^{33}	[29]	
$pp \to \pi^+\pi^+$	I–IV	282	7.2×10^{31}	[30]	A part of SK IV data
$pn \to \pi^+\pi^0$	I–IV	282	1.7×10^{32}	[30]	A part of SK IV data
$nn \to \pi^0\pi^0$	I–IV	282	4.0×10^{32}	[30]	A part of SK IV data
$np \to e^+\nu$	I–IV	273	2.6×10^{32}	[25]	A part of SK IV data
$np \to \mu^+\nu$	I–IV	273	2.2×10^{32}	[25]	A part of SK IV data
$np \to \tau^+\nu$	I–IV	273	2.9×10^{31}	[25]	A part of SK IV data
$pp \to K^+K^+$	I	92	1.7×10^{32}	[31]	
$n \to \bar{n}$	I–IV	373	3.6×10^{32}	[32]	

Fig. 17. Summary of the latest nucleon decay searches in SK. X is an invisible, massless particle.

Currently, in addition to updating the analysis of these decay modes, we are also searching for decay modes that have not previously been searched for in SK, such as a neutron decay to a charged lepton and a charged kaon. Attempts to reconstruct events using new software techniques such as machine learning have also begun.

D. Future experiments

The Hyper-Kamiokande (HK) [33] is a third-generation water Cherenkov detector currently under construction in Kamioka, Japan. The HK detector will use a 187 kiloton water target, about 8 times that of SK. The experiment is expected to begin operations in 2027 and to improve on nucleon decay searches at SK by an order of magnitude or more using similar analysis technique. HK will be instrumented with improved 50 cm PMTs with increased quantum and collection efficiencies, resulting in twice the photon detection efficiency of the sensors used in SK. The HK PMTs will also have about half the timing resolution for single photoelectron signals. Both of these features positively impact searches for nucleon decay at HK. Notably, atmospheric neutrino backgrounds can be reduced by 30% relative to SK's achievement. HK's 3σ discovery potentials for the benchmark modes are shown in Fig. 18.

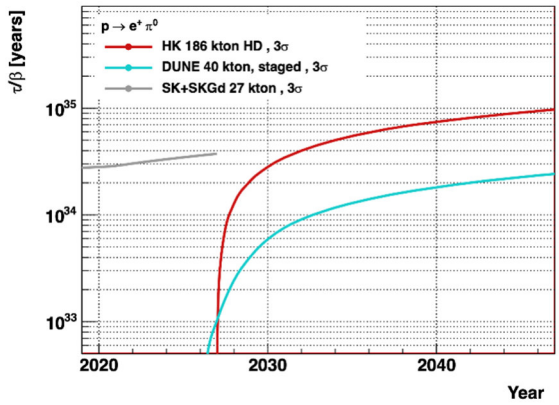

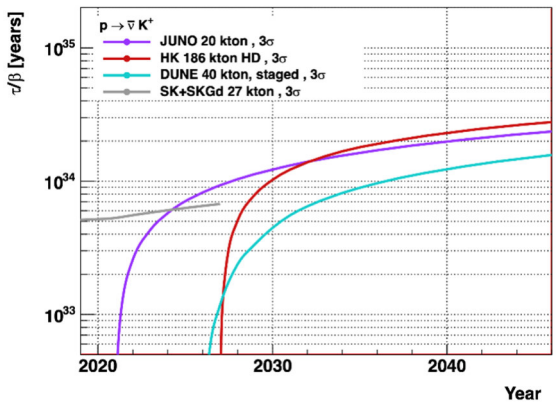

Fig. 18. 3σ discovery potentials for the benchmark modes for HK [33], DUNE [34], and JUNO [35].

For the $p \to e^+\pi^0$ and $p \to \bar{\nu}K^+$ modes, a lifetime less than 6×10^{34} years and 2×10^{34} will lead to a 3σ detection after 10 years, respectively.

Fig. 19 summarizes the currently planned nucleon decay search experiments.

Experiment	Detector technology	Fiducial volume [kiloton]
HK	Water Cherenkov	~190
DUNE	Liquid argon TPC	~40
JUNO	Liquid scintillator	~20
THEIA	Water-based liquid scintillator	~100

Fig. 19. Future nucleon decay search experiments [9].

The sensitivity of the future experiments to the benchmark decay modes is shown in Fig. 7. These detectors have the capability to improve the existing limits on nucleon lifetime by up to two orders of magnitude. A broad class of GUTs, both non-supersymmetric and supersymmetric, can be probed. Some of them predict an upper limit on the nucleon lifetime, which might be fully within reach of the future experiments.

III. SUMMARY

Testing baryon number violation (BNV) is an essential and high priority objective of particle physics. The discovery of BNV will be an unambiguous signal of new physics, and therefore, it is important to search for as many BNV channels as possible.

Nucleon decay searches at SK are on-going. We have not yet found any evidence and continue to provide the most stringent lifetime limits. We have prospects of sensitivity improvements by expanding fiducial volume, sophisticated event reconstruction algorithms, and other improvements. We are also searching for new decay modes.

Future experiments will be conducted using different detector technologies. Confirmation of the observation of the BNV signal using different technologies would provide powerful evidence of physics beyond the SM of particle physics.

ACKNOWLEDGMENT

I would like to thank a number of people for their help in compiling this summary. In particular I would like to thank: Gianfranca De Rosa (University of Naples Federico II and INFN Naples) for giving me the opportunity to present this

overview of nucleon decay. Ed Kearns (Boston University) for his helpful advice in the preparation of this document. I highly recommend checking out his 2022 SLAC Summer Institute lecture "Experimental Studies of the Grand Unification" [36] as it contains more topics which I could not cover including the history of the development of theories and experiments and the nuclear modeling of proton decay in ^{16}O. I also thank Neil McCauley (The University of Liverpool) and Makoto Miura (ICRR, The University of Tokyo) who reviewed this document and provided many useful comments and corrections. I would like to gratefully acknowledge the Super-Kamiokande collaboration, of which I am a member, for 27 years of work on nucleon decay that have informed the writing of this document. Finally, I would like to thank ICRR for funding me to attend NNN23.

REFERENCES

[1] https://pdg.lbl.gov/2023/reviews/rpp2022-rev-guts.pdf

[2] Phys. Rev. Lett. 32, 438 (1974).

[3] Phys. Rev. D 24, 1681 (1981); Nucl. Phys. B193, 150 (1981); Phys. Lett. 105 B, 439 (1981); Z. Phys. C 11, 153 (1981); Nucl. Phys. B 196, 475 (1982); Phys. Rev. D 25, 3092 (1982).

[4] arXiv:hep-ph/9302260.

[5] Annals Phys. 93, 193 (1975).

[6] Sov. Phys. Usp. 34 (5), May 1991.

[7] Phys. Rept. 79, 1 (1981); Front. Phys. 54, 1 (1982); Comput. Phys. Commun. 192, 166 (2015); PTEP 2016, 4, 043B02 (2016).

[8] Phys. Lett. 112 B, 133 (1982); Nucl. Phys. B 202, 43 (1982).

[9] arXiv:2203.08771v2.

[10] Phys. Rev. D 59, 052004 (1999); Phys. Lett. B 220, 308 (1989); Z. Phys. C 50, 385 (1991); Phys. Rev. D 36, 1990 (1987).

[11] Nucl. Instrum. Methods Phys. Res. A 501, 418 (2003); Nucl. Instrum. Methods Phys. Res. A 737, 253 (2014).

[12] http://hep.bu.edu/~superk/pdk.html

[13] Nucl. Instrum. Methods Phys. Res. A 433, 240 (1999).

[14] Phys. Lett. B 374, 238 (1996).

[15] Phys. Rev. D 96, 012003 (2017).

[16] Nucl. Instrum. Methods Phys. Res. A 1027, 166248 (2022).

[17] Phys. Rev. D 102, 112011 (2020).

[18] Phys. Rev. D 77, 032003 (2008).

[19] Phys. Rev. D 74, 072003 (2006).

[20] Phys. Rev. D 102, 112011 (2020).

[21] Phys. Rev. Lett. 113, 121802 (2014).

[22] Phys. Rev. D 96, 012003 (2017).

[23] Phys. Rev. D 101, 052011 (2020).

[24] Phys. Rev. Lett. 113, 101811 (2014).

[25] Phys. Rev. Lett. 115, 121803 (2015).

[26] https://indico.cern.ch/event/754031/contributions/3578554/attachments/1928723/3199003/BLV19-SKpdecay-191018-upload.pdf

[27] Phys. Rev. D 106, 072003 (2022).

[28] Phys. Rev. D 72, 052007 (2005).

[29] arXiv:1811.12430.

[30] Phys. Rev. D 91, 072009 (2015).

[31] Phys. Rev. Lett. 112, 131803 (2014).

[32] Phys. Rev. D 103, 012008 (2021).

[33] arXiv:1805.04163.

[34] arXiv:2002.03005.

[35] arXiv:1508.07166.

[36] https://indico.slac.stanford.edu/event/7118/contributions/4140/attachments/2022/5192/Kearns-Unification-Experiments.pdf